Polymer Degradation and Stability 218 (2023) 110551

Contents lists available at ScienceDirect

Polymer Degradation and Stability

journal homepage: www.journals.elsevier.com/polymer-degradation-and-stability

Enhancing PANox fiber properties through controlled oxidation and tensioning: A study on shrinkage inhibition and structural analysis

Luca Zoli [a,*], Francesca Servadei [a], Francesca Cicogna [b], Serena Coiai [b], Lucia Calucci [b,c], Claudia Forte [b,c], Diletta Sciti [a], Elisa Passaglia [b,*]

[a] CNR-ISSMC (former ISTEC), Institute of Science, Technology and Sustainability for Ceramics, Via Granarolo 64, Faenza 48018, Italy
[b] CNR-ICCOM, Institute of Chemistry of OrganoMetallic Compounds SS Pisa, Via Moruzzi 1, Pisa 56124, Italy
[c] CISUP, Center for Instrument Sharing, University of Pisa, Via Santa Maria 53, Pisa 56126, Italy

ARTICLE INFO

Keywords:
PAN
PANOX
Stabilization
Tensile strength
ATR-IR
Solid state NMR
TGA-DSC
Elongation
Elastic modulus

ABSTRACT

PANOX fiber is a unique organic material used in high-performance applications such as automotive and aeronautics. It is a non-flammable, infusible, and non-drip fiber, obtained from the controlled oxidation of PAN. During this process, fibers tend to shrink. The resulting chemical composition and mechanical properties of the fiber are dependent on the time and temperature of the process, as well as on the tension applied to the fiber during oxidation. In this work, it was questioned whether fiber shrinkage could be prevented by applying tension to the bundle of fibers during the stabilization process and whether the effect of fiber length variation on the chemical structure and mechanical properties of PAN fibers could be studied. Chemical reactions were investigated by differential scanning calorimetry coupled with thermogravimetric analysis, Fourier-transform infrared spectroscopy, solid-state nuclear magnetic resonance spectroscopy, while strength and Young's modulus were determined by tensile tests. Results unravel a tension-applied, stabilization-process trade-off: enhanced stress reduces the yield of cyclization and dehydrogenation reactions. Fiber elongation inhibits these processes but boosts tensile strength and elastic modulus, particularly improving Young's modulus, however, it had a marginal influence on elongation at break. When the shrinkage of fibers was about 30 % (no stress applied) the tensile strength and Young's modulus were found to be the lowest values, 130 MPa and 4 GPa, respectively. The best compromise was found when the shrinkage was kept to about 5 %, resulting in improved strength of approximately 175 MPa and a modulus of 5 GPa. Therefore, effective tension management allows precise adjustment of PANOX fiber chemistry and mechanical properties, enabling tailored product design for diverse applications.

1. Introduction

PANOX is an oxidized polyacrylonitrile (PAN) fiber and is the industry standard when it comes to fire-retardant textile fibers because it is a non-flammable, infusible and non-dripping organic fiber. PANOX can be used in many different industries (mainly in automotive and aircraft sectors) as an effective fire and heat protective fiber for textiles.

The LOI (Limiting Oxygen Index) value of PANOX, higher than 45 %, is considerably larger than that of other fibers and corresponds to the combustion class S-a according to standard DIN 66,083. PANOX is generally produced by thermal stabilization reactions of polyacrylonitrile (PAN) copolymers in atmospheric oxygen at temperatures ranging from 180 °C to 270 °C [1]. This stabilization/oxidation step leads to an infusible and non-flammable partially cyclized polymeric ladder structure due to further polymerization (cross-linking process) of the nitrile side groups, accompanied/preceded by dehydrogenation reactions and uptake of oxygen from the atmosphere, according to a well-discussed process reported in the literature (Fig. 1) [2].

The extent of cyclization, dehydrogenation and oxidation reactions depends on the experimental conditions, mainly the temperature and time of reaction, and on the structure of pristine PAN copolymers, which generally contain small quantities of vinyl monomers, as vinyl acetate, itaconic anhydride/esters, and methyl methacrylate, to optimize the process extent and final thermomechanical features of PANOX [2–5].

In the industrial stabilization method, the precursor tow continuously passes through a furnace divided into several zones with increasing temperature gradient for the purpose of an ensuring low cost and high efficiency. The stretching applied to the fibers in the different

* Corresponding authors.
E-mail addresses: luca.zoli@cnr.it (L. Zoli), elisa.passaglia@pi.iccom.cnr.it (E. Passaglia).

https://doi.org/10.1016/j.polymdegradstab.2023.110551
Received 15 September 2023; Received in revised form 29 September 2023; Accepted 2 October 2023
Available online 3 October 2023

zones is achieved by controlling the speed difference between the feed and the take-up rollers.

Regarding the thermal treatment, processability of PAN fibers is enhanced at temperatures exceeding the glass transition temperature (Tg), commonly above 140 °C [6]. In this temperature region, the PAN precursor is partially softened, and this is the point where an improvement in fiber orientation can be achieved, while tension assists the stabilization process and leads to enhanced molecular alignment in the fibers.

Molecular structure is affected by several reaction pathways that transform the polymer backbone of fused heteroaromatic structures; furthermore, the presence of atoms such as residual hydrogen, nitrogen and oxygen can lead to crosslinking, and thus to higher carbon yields and an improved structure upon carbonization [7,8]. During the stabilization process, physical and chemical transformations occur that result in changes in fiber color (from white to black) and length. The latter is determined by three phenomena, namely entropic shrinkage, creep, and chemical shrinkage. The entropic shrinkage is the result of constrained oriented polymer chains returning to a random spiral configuration, while creep is a heat-activated phenomenon that depends on temperature, time and applied stress. These three parameters can be adjusted to prevent entropic shrinkage and maintain the orientation arising from the spin treatment. However, the application of very high stress values during stabilization can adversely affect the preferential orientation required for the cyclization reaction, leading to bond failure and thus compromising mechanical properties. Chemical shrinkage is the result of exothermic chemical reactions during the stabilization process that lead to the formation of cyclic ladder polymers, and it has been shown that it can be used as a measure of the progress of the nitrile cyclization reaction. The rate and extent of shrinkage depend on factors such as atmosphere, stabilization temperature, applied tension, elongation of the precursor fiber during the spinning process, and heating rate. The effect of different stretching on the structural evolution of PAN fibers during the stabilization stage is significant. This determines the formation and orientation of the cyclized structures, thus affecting the mechanical properties of the final PANOX fibers [9]. Although several works on this topic have attempted to correlate the tensile force exerted during stabilization treatments with the conversion of PAN to PANOX, the multiple mechanisms that alter molecular structures have not yet been elucidated [10–12].

As far as we know, no basic studies have been conducted to understand what happens to the cyclization and dehydrogenation reactions when the fiber is overstretched. The aim of this study is to provide new insight into the correlation between fiber stretching and the extent of cyclization, dehydration, oxidation in the stabilization process and resulting mechanical properties.

Keeping all the other experimental parameters constant, PAN fibers were heat treated in air up to 250 °C by applying different stress values to the bundle.

The extent of cyclization, dehydrogenation and oxidation reactions of the resulting PANOX was evaluated by solid-state nuclear magnetic resonance (SS-NMR) and attenuated total reflectance Fourier-transform infrared (ATR FT-IR) analyses together with thermogravimetric analysis (TGA) and differential scanning calorimetry (DSC) measurements, whose results are compared with those of starting PAN fibers. Finally, the influence of tension during the oxidative stabilization process on the tensile strength and Young's modulus of the resulting PANOX fibers was evaluated.

2. Experimental

2.1. Materials

Polyacrylonitrile (PAN) copolymer fiber yarns were composed of 96 % acrylonitrile, 3 % methyl acrylate, and 1 % itaconic acid (filament count: 0.5 K, dtex: 1.73 g/m, breaking tenacity: 1.32 cN/dtex, supplier: MAE S.p.A., Italy). The PAN fibers were not subjected to any treatment prior to stabilization.

2.2. Sample preparation

A lab-scale experimental setup (batch process) was designed to simulate the industrial process in a discontinuous mode in order to screen several conditions at the same time. The preparation of samples was carried out through the manufacturing of a tailored tool to unroll and cut the commercial tow. Our idea was to realize a loop-shaped sample and apply a certain tension value to the specimen by hanging it on a frame from one end and hooking a weight to the other end (see sketch in support information, Fig. S1). In this way, the specimen was kept under constant tension simulating the tension applied by the driven

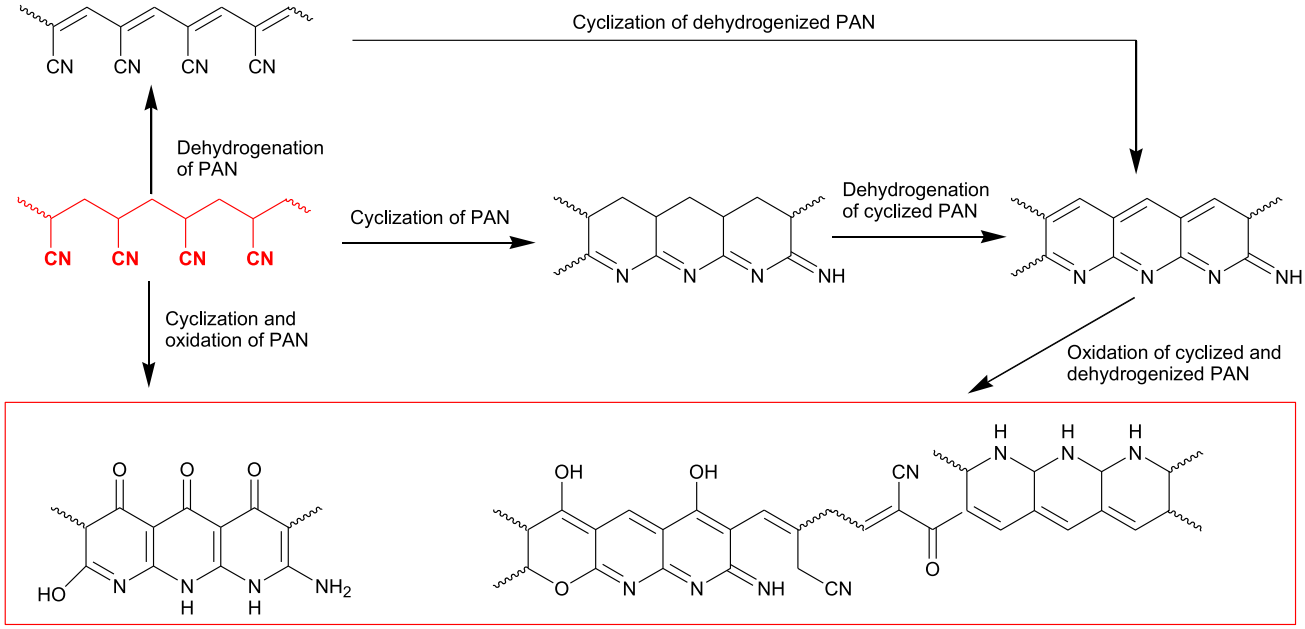

Fig. 1. Structural changes of carbon fiber during the stabilization/oxidation process (reactions with different occurrence order).

rollers in the continuous industrial process. Our method, with only a few meters of a bundle, is able to provide multiple samples characterized by different applied tension values in one batch (heat treatment). Detailed description of sample preparation is reported in the supporting information. More than one hundred specimens were prepared in this study and stretched with tensile forces from 0.01 N to 7.3 N. Among them, four specimens were selected to represent the selected four case studies: free shrink, controlled shrinkage, no shrinkage and creep elongation. In this work, pristine PAN fibers (not stabilized) and stabilized PANOX fibers were labelled as PAN and PX, respectively. Samples PX were numbered from 1 (no applied load) to 4 depending on applied tensile loads.

2.3. Thermo-oxidative stabilization

The same stabilization treatment was carried out for all specimens through a series of consecutive thermal ramps in air inside an electric furnace (KL 40/12S, Nannetti s.r.l., Italy) to a maximum temperature of 250 °C following the steps described in Table 1.

2.4. Microstructural characterization

For both pristine and stabilized fibers, the following properties were analyzed:

- Bulk density was determined by helium pycnometer (AccuPyc II 1340, Micromeritics, US). The analyses were performed according to EN ISO 1183–3, carrying out ten purging cycles with He of the chamber (1-cm^3 nominal cell volume) before the measurement. The value obtained is an average of 15 measurements.

- Linear density, D_l, was calculated by Eq. (1):

$$D_l = A * \rho S \quad (1)$$

where A is the cross-section area of the tow, ρ is the density, and S is the normalizing factor to the unit dtex [13].

- The mean area of the fibers was determined through image analysis using ImageJ software on micrographs collected by a digital microscope (RH-2000, Hirox, Japan), by converting optical images of sample cross sections in binary images and determining fiber average area through the "analyze particle" plug-in. Consequently, diameters of fibers and their linear densities were calculated. The micrographic specimens were obtained embedding the tow kept in tension in epoxy resin, thanks to homemade silicone molds, which were designed and manufactured for this purpose (see supporting information Fig. S2a,b). The flat surface of as-obtained specimens, exposing fiber sections (Fig. S2c), was polished using a semiautomatic polishing machine (Tegramin-25, Struers, Italy), washed with solvents in an ultrasonic bath and finally cleaned with a plasma cleaner (Colibrì Plasma RF 50 KHz, Gambetti, Italy). In this way, the bundle cross-section resulted more regular compared to that of a loose yarn (Fig. S2d,e) due to fiber alignment, making the microscope analysis more reliable.

Table 1
Thermal stabilization cycle with detail of heating steps: starting temperature and final temperatures, heating rate and holding time at the target temperature.

Heating steps n°	Initial temperature (°C)	Final temperature (°C)	Heating rate (°C/h)	Holding time (min)
1	25	220	150	0
1	220	230	70	10
2	230	235	25	5
3	235	240	25	10
4	240	245	25	25
6	245	250	25	20

2.5. Spectroscopic analyses

2.5.1. ATR FT-IR

Attenuated Total Reflection Infrared (ATR FT-IR) spectra were recorded with a Fourier Transform spectrometer (Spectrum Two, PerkinElmer, USA) equipped with a diamond crystal. Spectra were registered over the wavenumber range of 650–4000 cm^{-1} with a resolution of 4 cm^{-1} using 16 scansions. Deconvolution of the FT-IR spectra was performed using the OriginPro software Peak assignment was performed according to the literature [14–16].

2.5.2. Solid state NMR

Solid state NMR (SS-NMR) experiments were carried out on a spectrometer (Advance Neo, Bruker, USA) working at 500.13 MHz for ^1H and at 125.77 MHz for ^{13}C, equipped with a 4 mm CP-MAS probe head. ^1H–^{13}C cross-polarization (CP) NMR experiments with magic angle spinning (MAS) were recorded under high power proton decoupling, with a 90° pulse length of 3.7 μs, a contact time of 2 ms and a recycle delay of 6 s. The spinning frequency was 12 kHz, and the spectra were obtained accumulating 4000 scans. ^1H MAS NMR spectra were recorded using a 90° pulse length of 3.7 μs and a recycle delay of 6 s; 40 scans were acquired and the spinning rate was 15 kHz.

To allow quantitation of the ^{13}C spectra, CP-MAS experiments with variable contact time were performed on samples labelled as PX1, PX2, PX3 and PX4. In this case, the number of scans was 400 and the contact time was varied from 50 μs to 10 ms, while the remaining experimental parameters were the same as above. All experiments were performed at 25 °C, controlling the temperature within 0.1 °C. The peak areas determined at the different contact times were used to calculate the cross-polarization time, T_{CH}, and the ^1H spin–lattice relaxation time in the rotating frame, ^1H $T_{1\rho}$, using Eqs. (1) and (2) in [17], thus allowing a quantitative comparison for the different signals. Deconvolution of the ^{13}C CP-MAS spectra was performed using the SPORT-NMR software [18]. Peak assignment was performed according to the literature [19].

2.6. Thermal characterization

2.6.1. TGA analysis

Thermogravimetric analysis (TGA) was performed using a Seiko Exstar 7200 TG/DTA instrument. PAN and samples PX (5 − 10 mg) were placed in alumina sample pans (70 mL) and runs were carried out at the standard rate of 10 °C min^{-1} from 30 °C to 700 °C under nitrogen flow (200 mL min^{-1}). T_{onset} and T_{infl} were determined by analyzing the TG curve (as the intercept temperature of the tangents before and after the degradation step) and DTG curve (as the maximum of the peak), respectively.

2.6.2. DSC analysis

Differential Scanning Calorimetry (DSC) measurements were performed on 5 − 10 mg samples under nitrogen atmosphere (nitrogen flow was 50 mL·min^{-1} for all the experiments) by using a Perkin-Elmer DSC-4000 differential scanning calorimeter thermal analyzer equipped with a 3 stage cooler able to reach −130 °C. Previously, the instrument was calibrated by using indium (m.p. 156.6 °C, DH = 28.5 J/g) and zinc (m.p. 419.5 °C). PAN and PX1 − PX4 samples were heated from 30 °C to 400 °C or 450 °C at 10 °C/min; onset temperatures related to dehydrogenation and cyclization reactions were calculated on the basis of the tangent to the starting peak with respect to the baseline and the related enthalpy values were referred to grams of starting fibers.

2.6.3. Tensile tests

Tensile tests [20] were carried out both on pristine PAN bundles and air-stabilized samples PX, according to ASTM D2256 standard [21].

Specimens of 285 mm in length were fractured with a gauge length of 170 mm and a crosshead speed (i.e. stretching rate) of 170 mm/min by using a universal testing machine (Z050, Zwick-Roell, Germany)

equipped with 1 kN screw grips. A small amount of twist is recommended before testing multifilament yarns [21] in order to hold the filament fibers together, guaranteeing the same tension, and to confine the failure region at gauge length of the specimen away from the grip region for avoiding premature failure. After several attempts, eight twists were given to PAN and PX samples. In addition, to ensure the occurrence of failure within the gauge length of the specimen, the use of end tabbing, which can transfer the clamping force to the specimen through shear action, was evaluated for these tests. A sketch and pictures of the preparation of taut specimens PX with plastic tabs (i.e. epoxy resin, hot glue: ethylene-vinyl acetate) at the ends [20,22] through a homemade silicone mold are reported in the supporting information (Fig. S3).

At least five samples were prepared and analyzed for each condition set to test the reproducibility of the methodology. Tensile modulus was evaluated from the initial slope of the tensile curve (linear part) and the reported values are averages of five tests.

3. Results and discussion

3.1. Microstructure of PAN and PANOX samples

The color of PAN fiber bundles changed, during thermal treating in air, from translucent white to yellow, orange, reddish brown, brownish black and eventually black (Fig. 2a).

A linear correlation was found between the applied force and the resulting strain measured on samples after stabilization, see Fig. 2b.

Four samples were selected for further characterizations (Fig. 2b): i. a sample stabilized without applying forces (PX1) showing a relevant shrinkage in length (−32 %), chosen as reference; ii. a sample displaying a controlled linear shrinkage of about 6 % (PX2); iii. a balanced sample that underwent near-zero (−0.2 %) length variation (PX3); iv. a stretched sample showing an elongation of ~6 % (PX4) .

The nominal stress applied during stabilization (constant fiber area was taken into account), some key physical and mechanical properties of pristine PAN fibers and selected PX samples are reported in Table 2.

The linear density of pristine PAN fibers (1.73 dtex) was found lower than PX1 (1.83 dtex) but higher than other samples (Table 2). The increase in density is generally attributed to the tighter packing of the molecular chains following the cyclization of the nitrile groups, as well as to the addition of oxygen in the oxidative processes. From the process point of view, this feature is generally controlled by both temperature and stabilization time.

Image analysis revealed a mean fiber cross-sectional area of pristine PAN fibers of about 142 μm^2 (Fig. S4), corresponding to an average diameter of about 13.5 μm (Table 2). As shown in Fig. S4b and c, PAN fiber size was rather homogeneous, with most of the fibers having a diameter ranging from 12.5 μm to 15 μm. Thermo-oxidative stabilization led to a fiber shrinkage of several microns in radial direction in all treated samples, as expected. Samples PX maintained their original shape but had smaller diameter and the external fiber surface appeared more wrinkled compared to that of pristine fibers (see Figs. 3 and S4).

The comparison of the cross-sectional areas of the stabilized fibers at the ends in contact with the hooks and at the center of the two bundles constituting the loop-shaped samples did not reveal substantial differences. Therefore, it can be safely stated that samples PX have been subjected to a homogeneous stress along their entire length. The average fiber diameter in PX samples decreased almost linearly with increasing the applied nominal stress (Table 2). For instance, an average fiber diameter of 12.5 μm was determined for PX1, and the minimum was reached for the stabilized sample PX4 with a diameter of 10.1 μm.

3.2. ATR FT-IR analysis

The spectrum of PAN shows the characteristic absorption modes of acrylonitrile polymers (Fig. 4a): 2940 cm^{-1} (stretching -CH_2), 2243 cm^{-1} (stretching -CN), 1452 cm^{-1} (bending -CH_2), 1070 cm^{-1} (stretching -C-CN); in addition vibrational bands ascribable to different acrylic comonomers are clearly observed: the -C=O stretching of carbonyl together with signals between 1300 and 960 cm^{-1} (indicated by asterisks in the Fig. 4a) suggest the presence of vinyl acetate and possibly methyl methacrylate in the backbone of PAN [15,16].

Samples PX show similar ATR FT-IR spectra (Fig. 4b). In particular, the characteristic peaks of PAN can no longer be observed, while bands indicating of the formation of cycles are clearly detected between 1600 cm^{-1} and 1370 cm^{-1}. Only the spectrum of sample PX1 (free to shrink) maintains weak signals attributable to CH stretching in the region between 2900 cm^{-1} and 2850 cm^{-1}. The main absorption at about 1570 cm^{-1} is due to the stretching of -C=N and -C=C- bonds, also in aromatic moieties. The band at 1720 cm^{-1} suggests the presence of carbonyl groups that may have formed during the cyclization and oxidation processes (in addition to the residual presence of comonomers). All spectra do not show the signal at 2240 cm^{-1}, indicating that the cyclization reaction or, in any case, reactions involving the -CN functionality

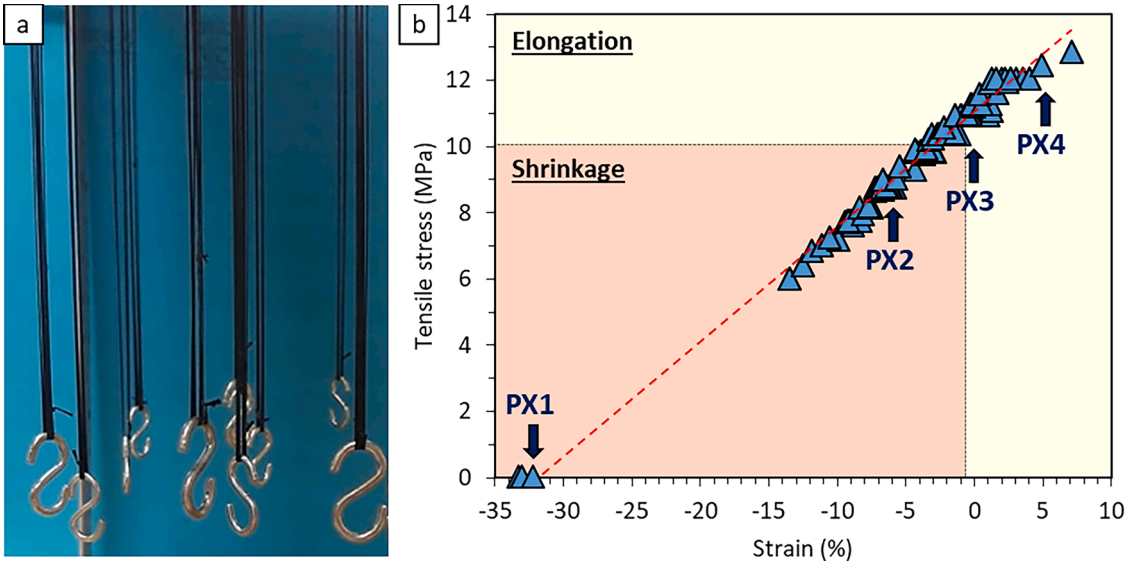

Fig. 2. PANOX samples: (a) Multifilament yarns; the color change from translucent white of pristine PAN to black is emphasized by blue background; (b) plot relating the change in length of PANOX fibers and stress applied during stabilization, highlighting selected samples PX1 – PX4.

Table 2
Applied stress and microstructural properties (i.e. strain, linear density, diameter, tensile strength, and elongation at break) of pristine PAN, selected PANOX fibers.

Sample	Applied stress MPa	Strain %	Linear density dtex (g/m)	Diameter μm	Tensile strength MPa	Elongation at break %	Young's Modulus GPa
PAN	none	none	1.73 ± 0.01	13.5 ± 0.05	320±20	16±2	5.4 ± 0.2
PX1	none	−31.8 ± 0.1	1.83 ± 0.01	12.5 ± 0.05	133±10	12±2	3.9 ± 0.1
PX2	9.0 ± 0.1	−5.9 ± 0.1	1.42 ± 0.01	11.0 ± 0.05	175±10	12±1	5.0 ± 0.2
PX3	11.0 ± 0.1	−0.2 ± 0.1	1.29 ± 0.01	10.5 ± 0.05	180±14	12±2	5.3 ± 0.5
PX4	13.0 ± 0.1	5.5 ± 0.1	1.19 ± 0.01	10.1 ± 0.05	210±15	12±2	6.2 ± 0.2

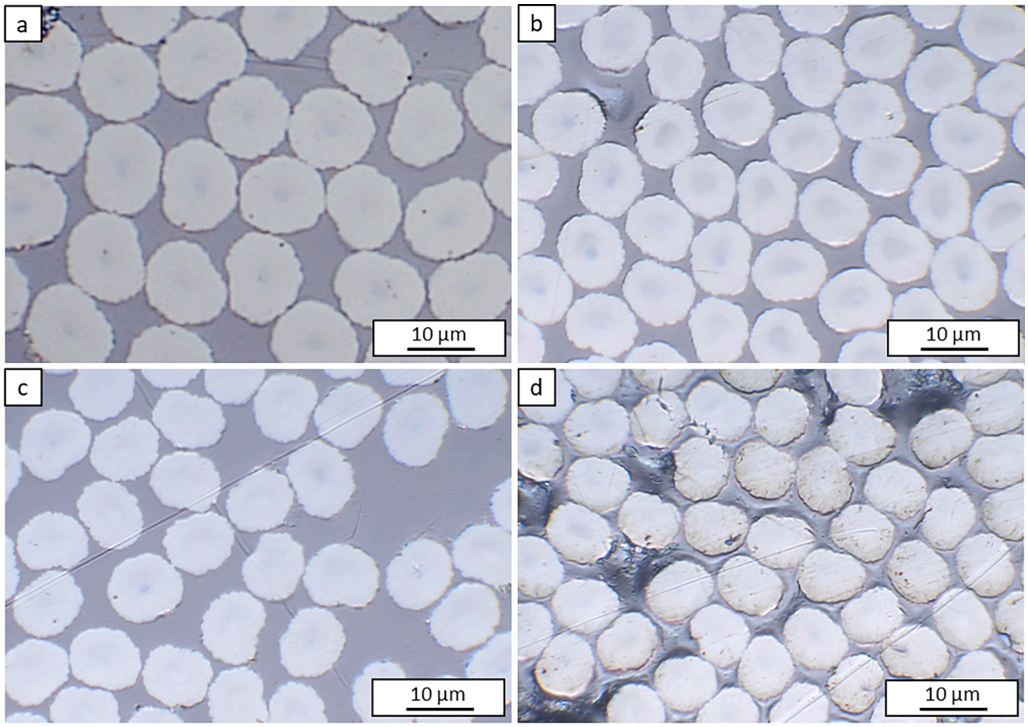

Fig. 3. Optical microscope pictures of polished cross section of samples PX: (a) PX1, (b) PX2, (c) PX3, (d) PX4.

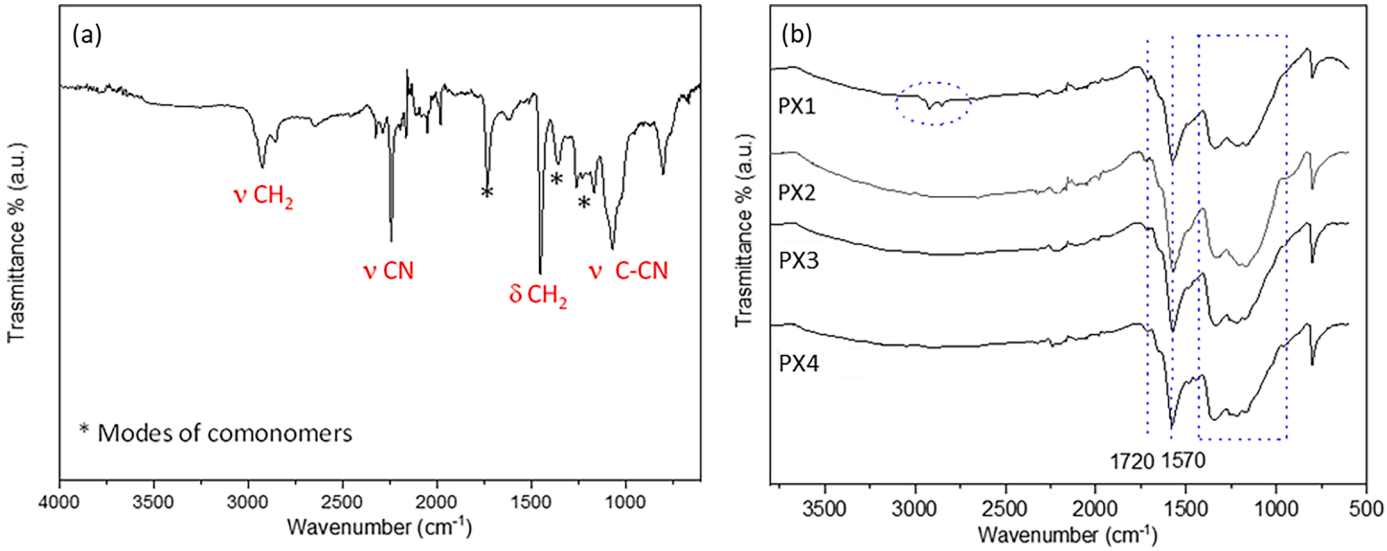

Fig. 4. ATR-IR spectra of: (a) PAN and (b) samples PX1 – PX4.

were probably almost complete, while the absorption range useful to estimate the dehydrogenation degree (at 1360 and at 1450 cm^{-1}) is partially hidden by bands relating to stretches –C=O, C=N, C=C, N-H [5,14,15].

To estimate the dehydrogenation index, a deconvolution of the absorption profiles in the range between 1760 cm^{-1} and 830 cm^{-1} was

carried out in order to determine the areas of the bands associated with the -CH (1350 cm^{-1}) and -CH_2 (1460 cm^{-1}) bending (see for example Fig. S5 in the supporting information where all the attributions were made following Zhao et al. [14]); the obtained values are reported in Table S1. Sample PX1 reveals a lower dehydrogenation index value in agreement with the observation of the -C-H stretching signals in the ATR FT-IR spectrum. For the other PX samples, the dehydrogenation index decreases with increasing applied stress, and is in any case higher than that of PX1, suggesting an effect of strain on the stabilization process.

3.3. SS-NMR analysis

The ^{13}C CP-MAS NMR spectra of the starting PAN fiber and the four PX samples are shown in Fig. 5.

The spectrum of the starting PAN material (Fig. 5a) shows the signals relative to the CH and CH_2 carbons at 28.8 ppm and 33.5 ppm, respectively, which are overlapped due to the broad linewidths, and to the CN carbon at 121.3 ppm, as reported in the literature [19]. The ^{1}H NMR spectrum of PAN, shown in Fig. S6 (supporting information), indicates the presence of a small amount of vinyl acetate and a spin finish resulting from the mixture of low molecular weight molecules already reported in the literature (Type B finish reported in [23]). In fact, the observation of very narrow signals in the ^{1}H NMR spectrum indicates that they are to be ascribed to very mobile components, as spin finishes, and not to monomeric units in the polymer backbone.

The ^{13}C CP-MAS NMR spectra of stabilized samples PX (Fig. 5b) show signals reported in the literature for PAN fibers stabilized in air [14,19], together with signals from unreacted PAN. Compared to the spectrum of PAN, there are new signals in the aromatic region, i.e. between 100 ppm and 165 ppm, and in the carbonyl region (170 – 180 ppm), which display first order spinning sidebands, the ones at low chemical shift underlying the signal centered at ~ 30 ppm, mainly ascribable to the CH and CH_2 carbons of unreacted PAN and to a less extent to the same type of carbons in non-aromatic cyclic units. The spectra of the four PX samples show the same peaks with different relative intensities of the signals. PX2 and PX3 display very similar relative intensities, except for the peak at ~ 138 ppm, which is slightly more intense for PX2.

To better highlight the differences among PX samples, spectral deconvolution was performed, which allowed the individual contributions of different structures to be distinguished (see the example reported in Fig. 5c). The assignment of the different peaks is reported in Fig. 5d.

Aromatization is clearly demonstrated by the signals at ~ 114 ppm, 138 ppm, and 154 ppm. The reaction with oxygen resulted in the formation of C=O groups on some of the aromatic rings, giving a signal at ~ 176 ppm. Given the absence of the representative signals expected at

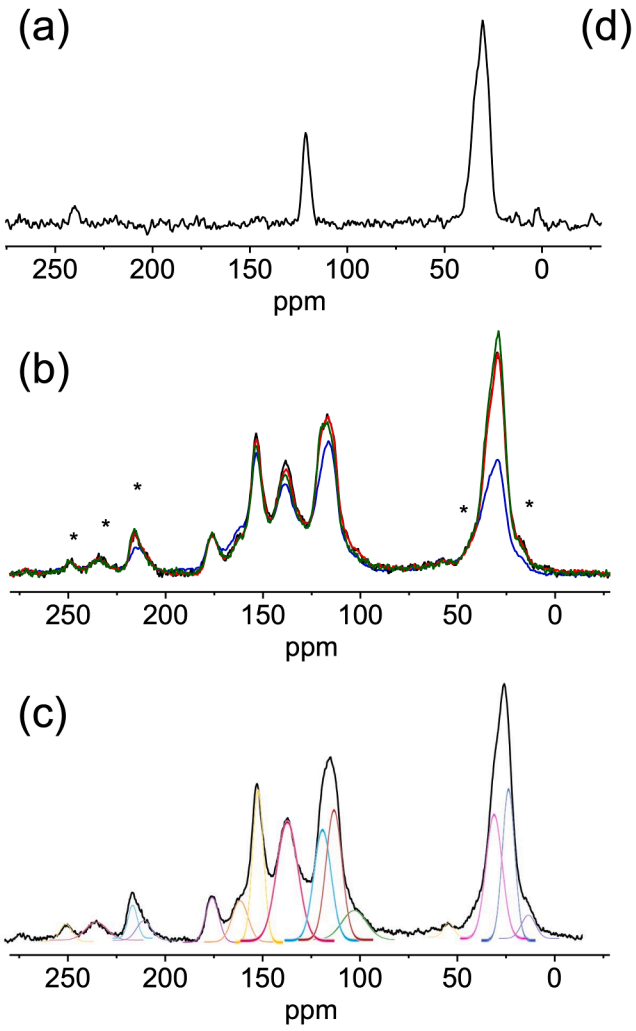

^{13}C chemical shift (ppm)	Functional group
30	
32	
108	
114	
117	
121	
128	
138	
145	
154	
163	
176	

Fig. 5. ^{13}C CP-MAS spectra of (a) PAN fiber, and (b) PANOX fibers (PX1 in blue, PX2 in black, PX3 in red, and PX4 in green), c) example of deconvolution of a PX spectrum (black asterisks indicate spinning sidebands); d) On the right is reported the table of assignment of the ^{13}C NMR peaks [19] (red asterisks indicates the carbon associated to the chemical shift value).

103 ppm and 180 ppm [19], C=O groups on adjacent rings were not formed or were present in very small amounts. Polyene structures are also present, as indicated by the signals at about 108 ppm, 117 ppm and 163 ppm. Signals at about 128 ppm and 145 ppm are ascribable to terminal pyridinic units [19]. The signal at 128 ppm could also arise from carbons in cross-linking structures [24], that at 145 ppm could be due to carbons in pyridinic groups bound to unreacted PAN or polyenic units, and that at 163 ppm could have contributions from non-aromatic cyclic structures or aromatic structures bearing a hydroxyl group [25]. The latter signal is more intense for PX1.

The quantitative analysis, although made difficult by the strong overlap of signals deriving from different functional groups, allowed the relative amounts of the main functional groups to be estimated. The aromatic units formed in the aromatization step represent the major fraction; these amount to 72 ± 5 % in PX1, while it is 60 ± 3 % in PX2, PX3, and PX4. Of these, ~22 % have C=O groups in the case of PX1, ~28 % in the case of PX2 and PX3, and ~32 % in the case of PX4. In PX1, approximately ~17 % of the aromatic units bear OH groups. Polyene units amount to 14 ± 2 % in all cases, whereas unreacted PAN fiber represents only 14 ± 2 % of units for PX1, 26 ± 2 % of units for PX2 and PX3, and 28 ± 2 % of units for PX4. The higher aromatization degree found for PX1 is in agreement with the high extent of shrinking.

Discrepancies between FT-IR and ^{13}C NMR results can be accounted for considering a core-skin structure for PANOX fibers, where unreacted PAN is mainly located in the core. This considered, ATR FT-IR, which mainly detects surface structures (the penetration depth into the material is typically below 2 μm, with the exact value determined by several parameters, see [26]), cannot reveal the presence of CN vibration bands from unreacted PAN, which is instead observable by NMR spectroscopy, which is a bulk technique.

3.4. Thermal characterization

In agreement with previous literature [2,27–29], DSC and TGA analyses carried out on PAN were used to evaluate the evolution of cyclization and dehydrogenation reactions as a function of temperature (Fig. 6).

The TGA curve shows four main steps (as numbered in Fig. 6) that can be associated with structural changes on the basis of the literature, as follows: (1) 200 °C – 270 °C: plateau due to cyclization and formation of the ladder structure with minimal weight loss; (2) 270 °C – 330 °C: weight loss due to dehydrogenation and heat generated by the cyclization reaction (see the DSC curve in black); (3) 330 °C – 480 °C: weight loss (52 %) due to volatilization of CH_4, NH_3, HCN, H_2O and CO_2; (4) 480 °C – 700 °C: a semi-plateau due to the stabilization of the ladder structure before the carbonization process starting at about 700 °C. The total residue at 900 °C is 41.80 %.

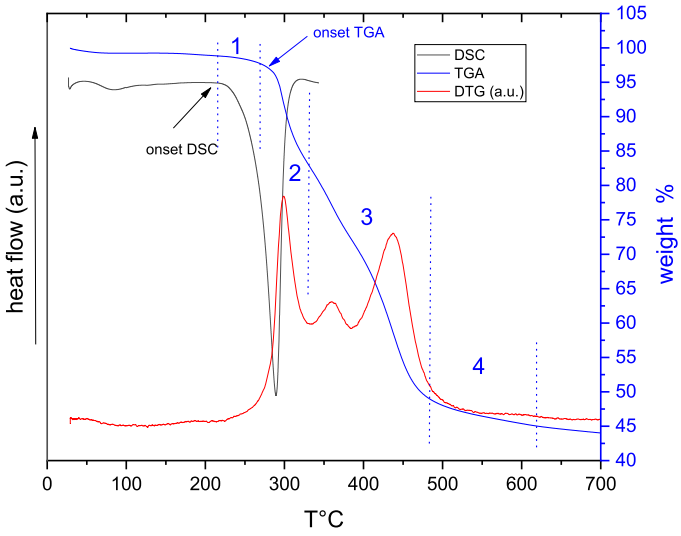

Fig. 6. TGA (blue), DTG (red) and DSC (black) curves for PAN. All analyses were conducted in nitrogen flow.

The DSC curve shows the heat associated with the starting reactions of the process: cyclization and dehydrogenation. Since the onset temperature (208 °C) of the observed transition (which has T_{peak}=289 °C and DH = 557 J/g) is lower than the onset temperature recorded in TGA, associated with mass loss, it can be deduced that the first phase of the stabilization process essentially involves cyclization reactions, at least in the absence of oxygen.

All PX samples were analyzed in the same way to qualitatively assess the effects of the stabilization process (carried out at increasing stress) on the two main reactions discussed above. The TGA analysis (Fig. 7) shows an initial step at very low temperatures (below 100 °C), associated with the volatilization of low molecular weight components (e.g. water), probably absorbed during or after the stabilization process (PANOX fibers are hygroscopic).

The TGA curves of the different samples are similar and show two following main steps with associated mass loss (between 300 °C and 470 °C the first, and at around 540 °C the latter), probably due to the completion of dehydrogenation reactions and the formation of aromatic structures with gas volatilization. The total mass loss (i.e. over the entire T range considered) increases with increasing the applied stress, from PX2 to PX4 (see Table 3), indicating a less complete process for the last sample.

The DSC analysis (Fig. S7 in the supporting information) confirms the presence of one or more absorbed volatile components, evidenced by an endothermic peak at low temperature. At higher temperature, the curves of the various samples feature a different behavior. While PX2 exhibits no further transitions, suggesting that cyclization and dehydrogenation are complete, samples PX1, PX3 and PX4 show exothermic peaks with relatively high onset (at about 265 °C) compared to that of the starting PAN. This result proves that I) for PX1 and PX3 and PX4 the stabilization process is not complete; II) considering the onset temperature value, the enthalpy content observed can be associated mainly with the completion of dehydrogenation and volatilization of CH_4, NH_3, HCN and other gases, even if residual cyclization occurrence cannot be completely excluded [30]. It is important to point out that the enthalpy associated with that transition is higher for PX4 (Table 3). This result, in agreement with other experimental evidence (IR and TGA), suggests that applied stress does affect the stabilization process and the applied stress value can be optimized in order to complete the stabilization process (keeping the other process parameters constant). In fact, the enthalpy values and thus of percentage of not reacted PAN (NRP), roughly estimated as reported in the footnote of Table 3) ascertain that these effects are most pronounced for stretched samples (third case study: PX4), for which a slowdown of or partial hindrance to the stabilization process occurred. Concerning PX1, it should be considered that this sample, having not been subjected to any stress, may have a different structure generated by the different contribution of the functional groups identified by NMR and ATR-IR. The residual DH value observed for this sample could result from the evolution with temperature of different amounts of cyclic (and non-cyclic) structures from those of the other samples, making it not perfectly comparable, at least for this type of investigation.

3.5. Tensile strength and elongation

Fig. 8 shows the stress-strain curves of all samples. Tensile strength of pristine PAN fibers is much higher than that of samples PX (Table 2), however among the latter a general increase in tensile strength with increasing the applied stress during stabilization (from PX2 to PX4) is highlighted. Moreover, while the elastic modulus is higher in PX4 with respect to PX2 and PX3, elongation at break is the same for all PX samples (Table 2).

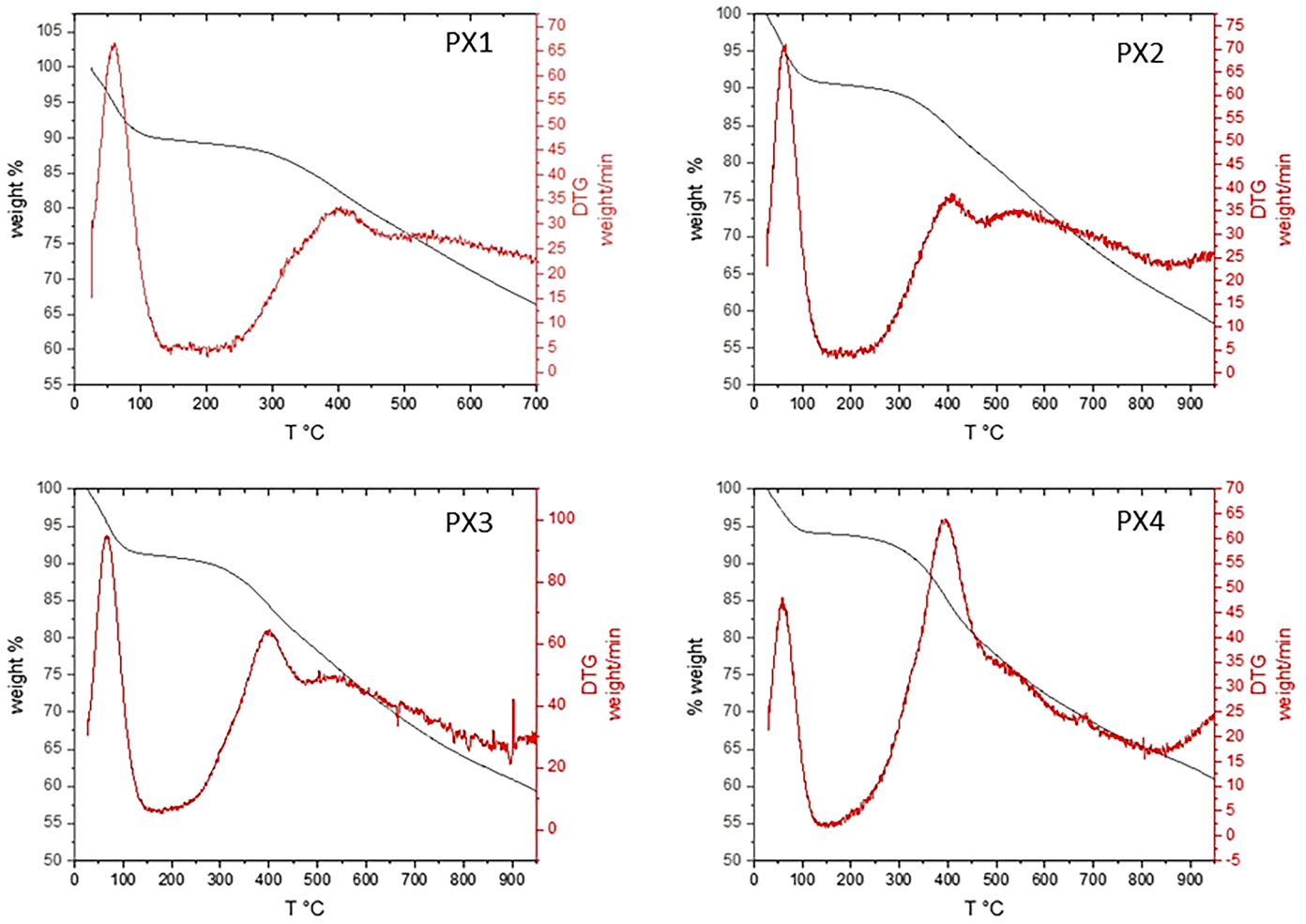

Fig. 7. TG and DTG curves of PX samples.

Table 3
Thermal characterization of PX samples.

Sample label	T peak DTG, °C	Yield @900 °C wt.%	wt. loss 150−480 °C %	T_{onset} DSC, °C	T_{peak} DSC, °C	-ΔH J/g	NRP
PX1	61/400/536	n.d.	12.3	268	341	68	13*
PX2	65/409/548	60.1	10.2	absent	absent	–	–
PX3	67/397/541	60.9	11.4	267	344	37	7*
PX4	60/392/~540	62.0	15.7	265	354	120	21*

NRP: not reacted PAN,.
* determined as a percentage based on the heat associated with the stabilization process (557 J/g).

The cohesive energy between the PAN polymer chains (intermolecular bonds) is responsible for the tensile strength of the fibers and the heat treatment in air greatly reduces it, causing the strength reduction observed in PANOX fibers. Other studies [31], focusing on the correlation of force vs increment of holding time during heat treatments, have shown that tensile strength decreases proportionally with increasing percentage of nitrile groups converted to imine cyclic moieties. This is indeed what is observed here, as NMR has detected an amount of residual nitrile groups in the order PX4>PX3≈PX2>PX1. Generally, tensile modulus mainly depends on the degree of molecular orientation in crystalline fibers. The increase in tensile modulus of sample PX4 suggests that a significant increment in molecular orientation in that fibers occurred due to the overstretching of the multifilament bundles during the process of stabilization.

4. Conclusion

In this work, commercial polyacrylonitrile (PAN) fibers were air stabilized at 250 °C controlling their shrinkage to evaluate the possible effect of the application of a tension load during stabilization on the extent of conversion into an aromatic ladder structure. We deliberately applied tension to the fibers until they reached their maximum elongation (without breaking) to investigate their structure and properties after stabilization.

The different stress levels tested indicated a linear decrease in shrinkage and ultimately a proportional increase in length upon application of an excessive tensioning.

Selected samples were subjected to ATR FT-IR, solid state NMR analyses and tensile tests to characterize the chemical structure and determine the tensile strength and Young's modulus of post-oxidized samples. The study demonstrates that relying solely on ATR FT-IR

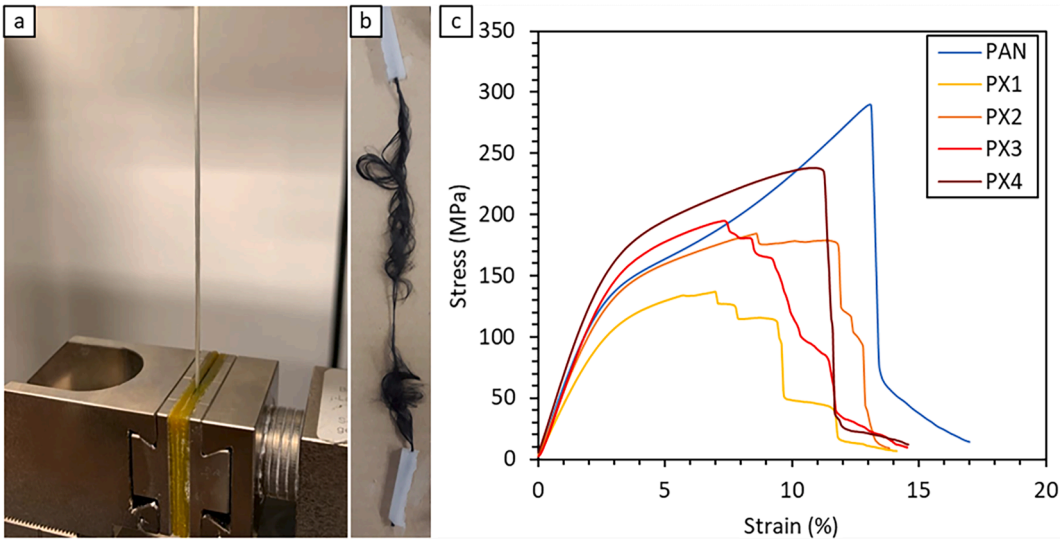

Fig. 8. Optical images of: (a) clamped PAN fiber bundle, (b) fractured PX specimen (with tabs) reported as an example of tensile fracture. (c) Stress-strain tensile curves of selected specimens: PAN (blue), PX1 (yellow), PX2 (orange), PX3 (red) and PX4 (brown).

analysis is inadequate for discerning material composition differences. This is due to its surface-focused nature, overlooking the core-skin effect within the material. The NMR and thermal analyses (TG-DSC) indicated that there is a trade-off between degree of reactions (cyclization and dehydrogenation) and increasing of applied stress during the stabilization process. Elongation of fibers hampers the dehydrogenation and cyclization processes but improves tensile strength and the elastic modulus. In our opinion, managing fiber tensioning offers a straightforward method to fine-tune the chemistry and mechanical properties of PANox fibers, enabling the production of tailored products for diverse applications.

CRediT authorship contribution statement

Luca Zoli: Conceptualization, Investigation, Methodology, Data curation, Writing – original draft, Funding acquisition. **Francesca Servadei:** Supervision, Investigation, Writing – original draft. **Francesca Cicogna:** Investigation, Visualization, Validation, Data curation. **Serena Coiai:** Investigation, Data curation. **Lucia Calucci:** Investigation, Formal analysis, Data curation. **Claudia Forte:** Investigation, Methodology, Validation, Writing – original draft. **Diletta Sciti:** Writing – original draft. **Elisa Passaglia:** Investigation, Methodology, Supervision, Validation, Visualization, Writing – original draft.

Declaration of Competing Interest

The authors declare that they have no known competing financial interests or personal relationships that could have appeared to influence the work reported in this paper.

Data availability

All data included in this study are available upon request by contact with the corresponding author.

Acknowledgments

The authors wish to thank MAE S.p.A., Italy for suppling indication on heat treatment cycle and suppling PAN fiber tow, Isacco Paci della Costanza (RWTH Aachen University) for his contribution in the preliminary investigation, G. Guarini (CNR-ISSMC) for Helium pycnometry analysis and C. Melandri (CNR-ISSMC) for optical microscope analysis and tensile testing.

This work was supported by Project MISE/INVITALIA Proposta di Contratto di Sviluppo Industriale CDS000750 (ai sensi dell'art 9 del Decreto del Ministro dello Sviluppo Economico del 09.12.2014) "Leonardo Automated Manufacturing Processes for cOmposites" Project Acronym LAMPO.

Supplementary materials

Supplementary material associated with this article can be found, in the online version, at doi:10.1016/j.polymdegradstab.2023.110551.

References

[1] J.E. Lee, Y.K. Chae, D.J. Lee, J. Choi, H.G. Chae, T.H. Kim, S. Lee, Microstructural evolution of polyacrylonitrile fibers during industry-mimicking continuous stabilization, Carbon 195 (2022) 165–173, https://doi.org/10.1016/j.carbon.2022.04.009. N Y.

[2] S. Arbab, A. Zeinolebadi, A procedure for precise determination of thermal stabilization reactions in carbon fiber precursors, Polym. Degrad. Stab. 98 (2013) 2537–2545, https://doi.org/10.1016/j.polymdegradstab.2013.09.014.

[3] Y. Sha, W. Liu, Y. Li, W. Cao, Formation mechanism of skin-core chemical structure within stabilized polyacrylonitrile monofilaments, Nanoscale Res. Lett. 14 (2019) 93, https://doi.org/10.1186/s11671-019-2926-x.

[4] E. Frank, D. Ingildeev, M.R. Buchmeiser, G. Bhat, 2 - High-performance PAN-based carbon fibers and their performance requirements. Structure and Properties of High-Performance Fibers, Woodhead Publishing, Oxford, 2017, pp. 7–30, https://doi.org/10.1016/B978-0-08-100550-7.00002-4.

[5] S. Nunna, M. Maghe, R. Rana, R.J. Varley, D.B. Knorr, J.M. Sands, C. Creighton, L. C. Henderson, M. Naebe, Time dependent structure and property evolution in fibres during continuous carbon fibre manufacturing, Materials 12 (2019) 1069, https://doi.org/10.3390/ma12071069 (Basel).

[6] A. Burkanudeen, G.S. Krishnan, N. Murali, Thermal behavior of carbon fiber precursor polymers with different stereoregularities, J. Therm. Anal. Calorim. 112 (2013) 1261–1268, https://doi.org/10.1007/s10973-012-2706-7.

[7] S. Soulis, J. Simitzis, Thermomechanical behaviour of poly[acrylonitrile-co-(methyl acrylate)] fibres oxidatively treated at temperatures up to 180°C, Polym. Int. 54 (2005) 1474–1483, https://doi.org/10.1002/pi.1871.

[8] J. Simitzis, S. Soulis, Correlation of chemical shrinkage of polyacrylonitrile fibres with kinetics of cyclization, Polym. Int. 57 (2008) 99–105, https://doi.org/10.1002/pi.2322.

[9] N. Meek, D. Penumadu, Nonlinear elastic response of pan based carbon fiber to tensile loading and relations to microstructure, Carbon 178 (2021) 133–143, https://doi.org/10.1016/j.carbon.2021.03.012. N Y.

[10] P. Gutmann, J. Moosburger-Will, S. Kurt, Y. Xu, S. Horn, Carbonization of polyacrylonitrile-based fibers under defined tensile load: influence on shrinkage behavior, microstructure, and mechanical properties, Polym. Degrad. Stab. 163 (2019) 174–184, https://doi.org/10.1016/j.polymdegradstab.2019.03.007.

[11] J. Choi, S.S. Kim, Y.S. Chung, S. Lee, Evolution of structural inhomogeneity in polyacrylonitrile fibers by oxidative stabilization, Carbon 165 (2020) 225–237, https://doi.org/10.1016/j.carbon.2020.04.027. N Y.
[12] G. Konstantopoulos, S. Soulis, D. Dragatogiannis, C. Charitidis, Introduction of a methodology to enhance the stabilization process of pan fibers by modeling and advanced characterization, Materials 13 (2020) 2749, https://doi.org/10.3390/ma13122749 (Basel).
[13] A.R. Bunsell, F. Matter, Handbook of Properties of Textile and Technical Fibres (Second Edition), Second Ed., Woodhead Publishing, 2018, p. iii, https://doi.org/10.1016/B978-0-08-101272-7.01001-4.
[14] J. Zhao, J. Zhang, T. Zhou, X. Liu, Q. Yuan, A. Zhang, New understanding on the reaction pathways of the polyacrylonitrile copolymer fiber pre-oxidation: online tracking by two-dimensional correlation FTIR spectroscopy, RSC Adv. 6 (2016) 4397–4409, https://doi.org/10.1039/C5RA24320C.
[15] I. Karacan, G. Erdoğan, A study on structural characterization of thermal stabilization stage of polyacrylonitrile fibers prior to carbonization, Fibers Polym. 13 (2012) 329–338, https://doi.org/10.1007/s12221-012-0329-z.
[16] E.V. Loginova, I.V. Mikheev, D.S. Volkov, M.A. Proskurnin, Quantification of copolymer composition (methyl acrylate and itaconic acid) in polyacrylonitrile carbon-fiber precursors by FTIR-spectroscopy, Anal. Methods 8 (2016) 371–380, https://doi.org/10.1039/C5AY02264A.
[17] C. Forte, A. Piazzi, S. Pizzanelli, G. Certini, CP MAS 13C spectral editing and relative quantitation of a soil sample, Solid State Nucl. Magn. Reson. 30 (2006) 81–88, https://doi.org/10.1016/j.ssnmr.2006.03.001.
[18] M. Geppi, C. Forte, The SPORT-NMR software: a tool for determining relaxation times in unresolved NMR spectra, J. Magn. Reson. 137 (1999) 177–185, https://doi.org/10.1006/jmre.1998.1662.
[19] X. Liu, W. Chen, Y. Hong, S. Yuan, S. Kuroki, T. Miyoshi, Stabilization of atactic-polyacrylonitrile under nitrogen and air as studied by solid-state NMR, Macromolecules 48 (2015) 5300–5309, https://doi.org/10.1021/acs.macromol.5b01030.
[20] R. Rypl, R. Chudoba, U. Mörschel, S.E. Stapleton, T. Gries, G. Sommer, A novel tensile test device for effective testing of high-modulus multi-filament yarns, J. Ind. Text. 44 (2015) 934–947, https://doi.org/10.1177/1528083714521069.
[21] ASTM D2256 / D2256M-21 Standard test method for tensile properties of yarns by the single-strand method, (2021). https://www.astm.org/d2256_d2256m-21.htm. Accessed February 15, 2023. doi:10.1520/D2256_D2256M-21.
[22] I. Mertová, E. Moučková, B. Neckář, M. Vyšanská, Influence of twist on selected properties of multifilament yarn, Autex Res. J. 18 (2018) 110–120, https://doi.org/10.1515/aut-2017-0018.
[23] S. Ghoshal, Y. Liu, P. Gulgunje, K. Gupta, H.G. Chae, J. Leisen, S. Kumar, Solid-state NMR study of spin finish of thermally treated PAN and PAN/CNT precursor fibers, J. Appl. Polym. Sci. 131 (2014), https://doi.org/10.1002/app.40734.
[24] B. Wang, C. Li, W. Cao, Effect of stretching on the orientation structure and reaction behavior of PAN fiber during the thermal stabilization, Mater. Res. Express. 8 (2021), 085603, https://doi.org/10.1088/2053-1591/ac19e9.
[25] Y. Xue, J. Liu, J. Liang, Correlative study of critical reactions in polyacrylonitrile based carbon fiber precursors during thermal-oxidative stabilization, Polym. Degrad. Stab. 98 (2013) 219–229, https://doi.org/10.1016/j.polymdegradstab.2012.10.018.
[26] Mirabella, Francis M., Jr., Internal Reflection Spectroscopy Theory and Applications. New York etc., M. Dekker, 1993. Print. Practical Spectroscopy 15. https://onesearch.unifi.it/primo-explore/fulldisplay/39sbart_almap7151732900003302/39UFI_V1.
[27] Q. Duan, B. Wang, H. Wang, Effects of stabilization temperature on structures and properties of polyacrylonitrile (PAN)-based stabilized electrospun nanofiber mats, J. Macromol. Sci. B 51 (2012) 2428–2437, https://doi.org/10.1080/00222348.2012.676415.
[28] H. Liu, S. Zhang, J. Yang, M. Ji, J. Yu, M. Wang, X. Chai, B. Yang, C. Zhu, J. Xu, Preparation, stabilization and carbonization of a novel polyacrylonitrile-based carbon fiber precursor, Polymers 11 (2019) 1150, https://doi.org/10.3390/polym11071150 (Basel).
[29] J. Moskowitz, J. Wiggins, Thermo-oxidative stabilization of polyacrylonitrile and its copolymers: effect of molecular weight, dispersity, and polymerization pathway, Polym. Degrad. Stab. 125 (2016) 76–86.
[30] P. Bajaj, T.V. Sreekumar, K. Sen, Thermal behaviour of acrylonitrile copolymers having methacrylic and itaconic acid comonomers, Polymer 42 (2001) 1707–1718, https://doi.org/10.1016/S0032-3861(00)00583-8 (Guildf).
[31] I. Karacan, G. Erdoğan, The role of thermal stabilization on the structure and mechanical properties of polyacrylonitrile precursor fibers, Fibers Polym. 13 (2012) 855–863, https://doi.org/10.1007/s12221-012-0855-8.